Available online at www.dergipark.gov.tr

INTERNATIONAL ADVANCED RESEARCHES
and
ENGINEERING JOURNAL

Journal homepage: www.dergipark.gov.tr/iarej

e-ISSN: 2618-575X

International Open Access

Volume 02
Issue 01

April, 2018

Research Article

Numerical investigation of combined effect of nanofluids and impinging jets on heated surface

Mustafa Kilic[a]*, Mahmut Yavuz[a], İbrahim Halil Yılmaz[b]

[a]*Department of Mechanical Engineering, Adana Science and Technology University, Adana, 01250, Turkey*
[b]*Department of Automotive Engineering, Adana Science and Technology University, Adana, 01250, Turkey*

ARTICLE INFO

Article history:
Received 02 March 2018
Revised 10 March 2018
Accepted 12 March 2018

Keywords:
Heat transfer
Multiple impinging jets
Nanofluids

ABSTRACT

Present study is focused on numerical investigation of heat transfer and fluid flow from a heated surface by using nanofluids and impinging jets. Effects of Reynolds number, different particle diameter and different types of nanofluids (TiO_2-water, CuO-water, NiO-water) on heat transfer and fluid flow were studied numerically. TiO_2-water nanofluid was used as a base coolant. Three impinging jets were used to cool the surface. It is obtained that increasing jet velocities from Ren/Re1=1-1.33-1.67 to Ren/Re1=1-1.20-1.40 causes an increase of 49.9% on average Nusselt number (ANN) but increasing jet velocities from Ren/Re1=1-1.20-1.40 to Ren/Re1=1-1.17-1.33 causes a decrease of 4.6% on ANN. Particle diameter from Dp=80nm to 10nm causes an increase of 2.9% on ANN. Using NiO-Water nanofluid causes an increase of 1% on ANN with respect to CuO and 2.8% with respect to TiO_2-water. Low Re k-ε turbulent model of PHOENICS CFD code was used for numerical analysis. Numerical results show a good approximation to experimental results.

1. Introduction

The jet cooling technique provides an important enhancement in heat transfer. Impinging jet technique can be used to boost up heating, cooling or drying processes on a selected surface. Impinging jets technic enhance heat transfer by increasing local heat transfer coefficient between the impinged fluid and a selected surface.

Suspension of solid particles which have 1-100 nm size in a base fluid called as nanofluid. Nanoparticles suspended in base fluid can expand thermal capacity of the fluid and also interactions and collisions between nanoparticles cause to increase in turbulence and turbulence intensity of the transition surface. Nanoparticles have 20% of their atoms on the particle surface, making them ready to heat transfer with high heat transfer coefficient. Nanoparticles provide another advantage which called as the particle mobility to nanofluids. Particle mobility causes micro-convection in the liquid due to its nano size and therefore increases heat transfer. Hence, they have a wide range of application in industry as microelectronics medicine and space research. Combination of the liquid jet impingement and the nanofluid technologies provides advantages of both and consequently improves the heat transfer significantly. This improvement means compact size and low weight which reduces the cooling system capital cost.

Many studies on nanofluid or impinging jet, can be found in the literature. Cakır M.T. [1] experimentally examined the thermal performance of the thermosiphon-type heat pipe which is using nanofluid as a working fluid. The nanofluid contained 2% by volume Al_2O_3. As a result, significant reduce on thermal resistance is obtained but a complete stabilization at thermal efficiency could not be provided. Sun et al. [2] searched the effect of a single jet using CuO nanofluid for heat transfer. It has been determined that when the nanofluid is used, a significant increase in heat transfer can be achieved compare with water. When a circular nozzle is used, a higher heat transfer coefficient is obtained compared to a square shaped nozzle, and the highest heat transfer is obtained when the jet angle is 90º. Teamah et al. [3] examined the heat transfer and flow structure for a flat plate by numerically and experimentally with different Reynolds numbers (Re = 3000-32000) and nanofluid volume ratios

* Corresponding author. Tel.: *+90 (322) 455 0000 - 2140*
E-mail address: mkilic@adanabtu.edu.tr
Note: This study was presented at International Advanced Researches and Engineering Congress 2017 (IAREC'17)

(φ= 0-10%) by using Al_2O_3 nanofluid. It has been observed that as volume fraction of nanoparticles in the fluid are increased, the heat transfer from the surface increases. Heat transfer coefficient can be increased by 62% when compared with the water. Qu et al. [4] Used Al2O3-water as working nanofluid in their experiment to investigate the thermal performance of a closed-loop vibrating heat pipe. As a result, they observed that the thermal resistance of the system decreased by 32.5% compared to pure water. Chien et al. [5] experimentally observed the application of nanofluid in the flat plate heat pipe. It was acquired that the use of nanofluid achieve 40% reduction in thermal resistance compared to pure water utilization. Kang et al. [6] determined that, when nanofluid which include 10 nm and 35 nm sized Ag nanoparticles is used, thermal resistance diminished by 50% and 80% compared to pure water respectively. Xuan and Li [7]. Prepared nanofluid that include Cu and they investigated heat transfer effect of nanoparticle volume fraction, heat transfer effect of particle diameter and heat transfer effect of particle geometry. As a result; it has been found that an increase of from 2.5% to 7.5% in the volumetric range causes an increase in the coefficient of thermal conductivity of nanofluid from 1.24 to 1.78. Shang et al. [8] studied the heat transfer characteristics of a closed-loop vibrating heat pipe with Cu-water nanofluid. They obtained that compared with pure water, the heat transfer capacity of the system increased by 83% when nanofluid was used. Manay et al. [9] have compiled recent studies which focusing on using of nanofluids in microchannel. As a result, nanofluids using in microchannel increases heat transfer, but the presence of nanoparticles causes an increase in pressure loss. Naphon et al. [10] investigated the heat transfer between the nanofluids that they built using titanium-ethanol and the closed two-phase thermosiphon. An increase of 10.6% on heat transfer was obtained by using nanoparticles, compared to ethanol using. Kilic et al. [11] examined the cooling of a flat plate by using impinging fluid air jet. It was observed that the mean Nusselt number increases by 49.5% when Reynold numbers is between 4000 and 10000. There are also some studies about alternative energy resources of [14-16]. As seen from literature there are some studies about impinging jets and nanofluids separately but researches of enhancing heat transfer by using nanofluids and impinging jets are required.

2. Numerical Model

Low Re k-ε turbulence model of PHOENICS CFD code was used for this numerical analysis. CFD simulation domain is shown in Figure1. Mesh structure is shown in Figure2.

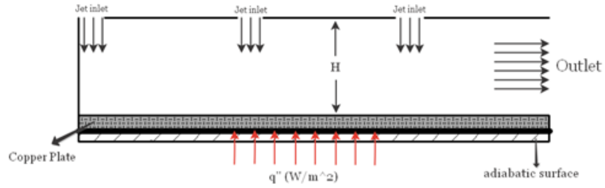

Figure 1. CFD simulation domain

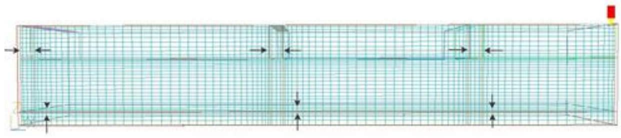

Figure. 2. Mesh structure

The continuity, Reynolds averaged momentum and time averaged energy equations governing 3-dimensional steady, flow of air with constant properties used for turbulent solutions can be written in the Cartesian coordinate system as follows:

Continuity equation:

$$\frac{\partial U_i}{\partial x_i} = 0 \tag{1}$$

Momentum equation:

$$\rho U_i \frac{\partial U_j}{\partial x_i} = -\frac{\partial P}{\partial x_j} + \frac{\partial}{\partial x_i}\left[\mu\left(\frac{\partial U_i}{\partial x_j} + \frac{\partial U_j}{\partial x_i}\right) - \rho\overline{u_i'u_j'}\right] \tag{2}$$

Energy equation:

$$\rho c_p U_i \frac{\partial T}{\partial x_i} = \frac{\partial}{\partial x_i}\left[k\frac{\partial T}{\partial x_i} - \rho c_p \overline{u_i'T'}\right] \tag{3}$$

All the boundary conditions used in the study are summarized in Table 1.

Table 1. Boundary Conditions

	U (m/s)	V (m/s)	W (m/s)	T (ºC)	k	ε
$W_{jet,inlet}$ (W_1,W_2,W_3)	U=0	V=0	W= W inlet	T=T_{inlet}	$(T_I W_{jet})^2$	$(C_\mu C_d)^{3/4}\frac{k^{3/2}}{L}$
Cu Plate	U=0	V=0	W=0	q"=q_{inlet}	k=0	$\frac{\partial \varepsilon}{\partial z} = 0$
Outlet	$\frac{\partial U}{\partial x} = 0$	$\frac{\partial V}{\partial x} = 0$	$\frac{\partial W}{\partial x} = 0$	T=T_{out}	$\frac{\partial k}{\partial x} = 0$	$\frac{\partial \varepsilon}{\partial x} = 0$
Front and Back wall	U=0	V=0	W=0	$\frac{\partial T}{\partial y} = 0$	-	-
Top wall	U=0	V=0	W=0	$\frac{\partial U}{\partial z} = 0$	-	-

It was used 96x15x34 (48960 elements) mashes for this application. Mesh structure was prepared according to flow conditions. In order to get more precise numerical results, we intensified mesh numbers in some region as jet inlet, surface of copper plate. Sweep number was studied between 400 and 2500 and cell number was also studied between 24 and 44. It is observed that numerical geometry was independent from sweep number and cell number when sweep number was 600 and cell number was 96x15x34. Verification of this modal with experimental results of Kilic [12] was shown in Figure3.

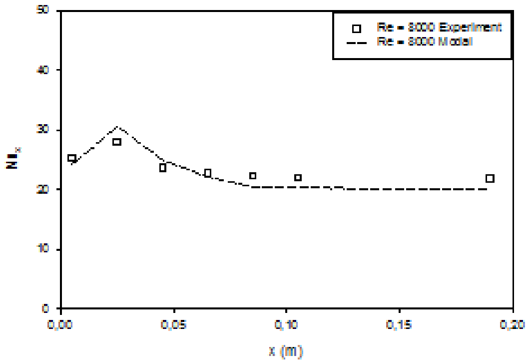

Figure 3. Verification of modal with experimental result

3. Date Reduction

The heat transfer from the surface will take place by convection, conduction and radiation.

$$Q_{convection} = Q_{total} - Q_{conduction} - Q_{radiation} \tag{4}$$

The total amount of heat to be given to the plate is;

$$Q_{total} = \frac{V^2}{R} \tag{5}$$

Where V is the voltage value of the power unit and R is the resistance of the heater. Here, the heat generated by the heater placed under the copper plate will be transmitted to the upper surface of the plate through the copper plate thickness by conduction, and as a result, the plate surface will be cooled by using nanofluid with impinging jet. Heat transfer by conduction along the plate

$$Q_{conduction} = \frac{-k_c.A_c.(T_{bottom} - T_{upper})}{L_c} \tag{6}$$

here, kc is the heat transfer coefficient of the copper plate, Ac is the copper plate surface area, and Lc is the copper plate thickness.

Thermal loses due to radiation;

$$Q_{radiaton} = \varepsilon.\sigma.A.F.(T_s^{\,4} - T_{bulk}^{\,4}) \tag{7}$$

Where ε is the copper plate emissivity, σ is the Stefan Boltzmann constant, A is the radiation surface area, T_s is the surface temperature, and T_{bulk} is the mean fluid temperature.

$$T_{bulk} = \frac{T_{in} + T_{out}}{2} \tag{6}$$

It is assumed that heat transfer with radiation is negligible in this study because surface temperature is under 573.15 K.

Heat transfer from surface with convection;

$$Q_{convection} = h.A.\Delta T \tag{7}$$

Where h is the heat transfer coefficient, A is the convection surface area, ΔT ($\Delta T = T_s - T_{bulk}$) is the difference between the measured surface temperature and the fluid mean temperature.

Nusselt number (Nu) is a dimensionless parameter indicating the ratio of heat transfer with conduction to h eat transfer with convection.

$$Nu = \frac{(Q_{convection}.D_h)}{(T_s - T_{jet}).k_{nf}} \tag{8}$$

Where T_s is the measured surface temperature, D_h is the hydraulic diameter, and k_{nf} is the coefficient of thermal conductivity of the nanofluid. Reynolds number (Re) is used to determine for forced convection whether the flow is laminar or turbulent. Reynolds number based on turbulent flow;

$$\mathrm{Re} = \frac{(\rho_{nf}.V_{jet}.D_h)}{(\mu_{nf})} \tag{9}$$

Where ρ_{nf} is the nanofluid density, V_{jet} is the jet velocity, and μ_{nf} is the nanofluid dynamic viscosity. The density of nanofluids is;

$$\rho_{nf} = (1-\varphi).\rho_{bf} + \varphi.\rho_p \tag{10}$$

Where ρ_{bf} is the base fluid (water) density, φ is the volumetric ratio of the nanofluid, and ρ_p is the density of the solid particles in the nanofluid. The volumetric ratio of nanoparticles is;

$$\varphi = \frac{1}{(1/\omega).(\rho_p - \rho_{bf})} \tag{11}$$

Where ω is the density difference between the fluid and the main fluid (water). The nanofluid specific heat is calculated from;

$$C_{p_{nf}} = \frac{\varphi.(\rho.C_p)_p + (1-\varphi).(\rho.C_p)_f}{(\rho_{nf})} \tag{12}$$

Where $Cp_{(p)}$ is specific heat of particle, $Cp_{(f)}$ is specific heat of base fluid. The effective thermal conductivity of nanofluid is calculated according to Corcione [13];

$$\frac{k_{eff}}{k_f} = 1 + 4.4\,\mathrm{Re}^{0.4}\,\mathrm{Pr}^{0.66}\left(\frac{T}{T_{fr}}\right)^{10}\left(\frac{k_p}{k_f}\right)^{0.03}\varphi^{0.66} \tag{13}$$

Where Re is the nanoparticle Reynolds number, Pr is the Prandtl number of the base liquid. k_p is the nanoparticle thermal conductivity, φ is the volume fraction of the suspended nanoparticles, T is the nanofluid temperature (K), T_{fr} is the freezing point of the base liquid.

Nanoparticle Reynolds number is defined as;

$$Re = \frac{2\rho_f k_b T}{\pi \mu_f^2 d_p} \tag{14}$$

Kb is the Boltzmann's constant. The effective dynamic viscosity of nanofluid;

$$\mu_{nf} = \mu_{bf} (1 + 2{,}5\,\varphi + 4{,}698\,\varphi^2) \tag{15}$$

4. Results and Discussions

In this section, numerical results were prepared for three parameters.

1) Effects of different Reynolds number rate for Rn/R1=1-1.33-1.67 to 1-1.17-1.33
2) Effects of TiO_2-water nanofluid with 25 nm sized particles for different particle diameter on heat transfer (D_p=10, D_p=25, D_p=40, D_p=80).
3) Effects of different nanofluids on heat transfer (TiO_2-water, Cu-Water, NiO-water).

Effects of variant Reynolds number

Numerical analysis was conducted for different water flow regime for Rn/R1=1-1.33-1.67 to 1-1.17-1.33 when particle diameter was 25µm and inlet temperature T_{inlet}= 20 ºC.

Table 2. Reynolds Numbers

	W_1(m/sn)	W_2(m/sn)	W_3(m/sn)	Re_1(jet-1)	Re_2(jet-2)	Re_3(jet-3)	Re_1/Re_1	Re_2/Re_1	Re_3/Re_1
1.phase	6	8	10	21440,42	28587,23	35734,03	1	1,33	1,67
2.phase	8	10	12	28587,23	35734,03	42880,84	1	1,25	1,5
3.phase	10	12	14	35734,03	42880,84	50027,65	1	1,2	1,4
4.phase	12	14	16	42880,84	50027,65	57174,46	1	1,17	1,33

Velocity vectors and Temperature contours for different Reynolds numbers are shown in Figure4 and Figure5.

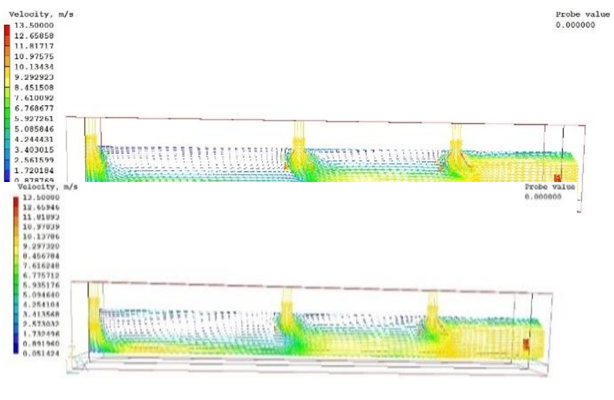

Figure 4. Velocity vectors for different Reynolds number (a) Rn/R_1=1-1.2-1.4 (b) Rn/R_1=1-1.17-1.33

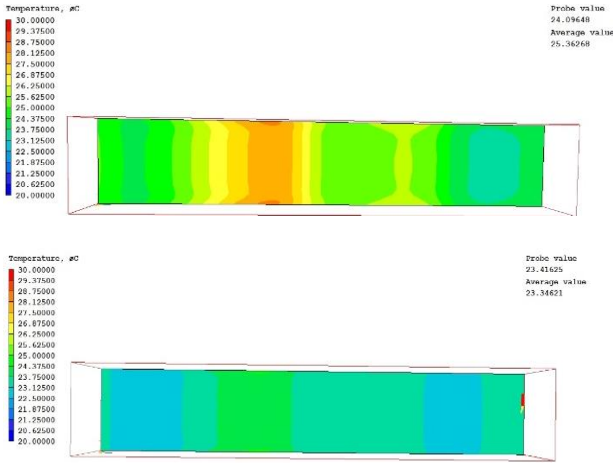

Figure 5. Temperature contours for (a) R_n/R_1=1-1.33-1.67 (b) R_n/R_1=1-1.2-1.4

It can be seen that increasing jet velocities from the first phase to the third phase local surface temperature decreases and local Nusselt number increases. But increasing jet velocities to the fourth phase causes an increase on surface temperature. The reason of this is that vortexes, which occurs at the bottom of the close side, enlarge while velocity on the first jet is increasing. And these vortexes reduce impinging effects and causes an increase on surface temperature and decrease on local Nusselt number. These effects continue at impinging region of second jet but effects of channel flow increases at this region. At the impinging region of the third jet there is not a significant difference between third and fourth phase because channel flow effects reduces impinging effects at this region by increasing velocities from third to fourth phase. So increasing jet velocities from the first phase to the third phase causes an increase of 49.9% on average Nusselt number but increasing jet velocities from the third phase to the fourth phase causes a decrease of 4.6% on ANN because of the effects of vortexes and the best velocity profile is the third phase. Local Nusselt number for different jet velocities are shown in Figure6

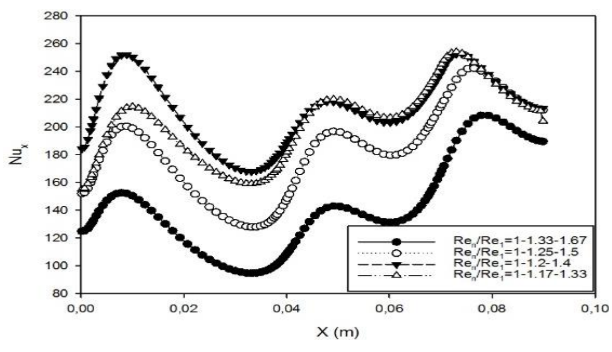

Figure 6. Local Nusselt number for different jet velocities

Effects of different nanoparticle diameters

Effect of different particle diameter (D_p=10, 25, 40, 80 nm) was analyzed numerically. It was observed that decreasing particle diameter from 80nm to 10nm causes a decrease on a surface temperature. Decreasing particle diameter from D_p=80nm to 10nm causes an increases of 2.9% between on ANN. These increase occurs 2.1% between D_p=40nm to 10nm. So increasing particle diameter from D_p=80nm to 40nm causes a slight decrease on ANN. So decreasing particle diameter causes an increase on ANN. Temperature contours on heated surface for different particle diameter are shown in Figure7.

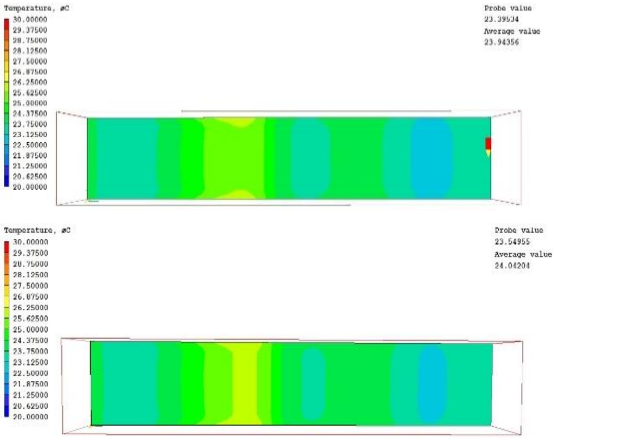

Figure 7. Temperature contours on surface for (a)D_p=10nm and (b)D_p=80nm

Variation of local Nusselt number for different particle diameter is shown in Figure8.

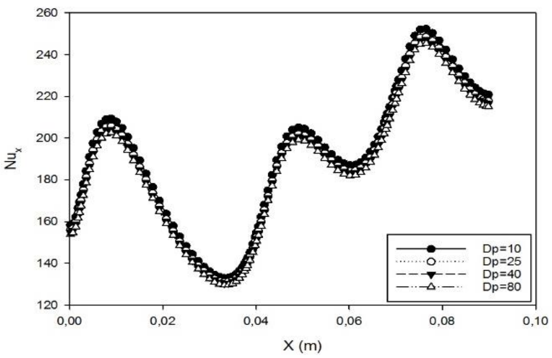

Figure 8. Local Nusselt number for different particle diameters.

Effects of different type of nanofluids

Numerical analysis is conducted for different type of nanofluids (CuO-water, TiO_2-water and NiO-water) with 25 nm particle size and volume fraction 2%. Calculated properties of nanofluids are shown in Table 2. Local Nusselt numbers on surface of heated place is shown in Figure9. For TiO_2-water, CuO-water and NiO-water. It was obtained that using NiO-Water nanofluid causes an increase of 1% on ANN with respect to CuO-Water and 2.8% with respect to TiO_2-water.

Table 3. Thermophysical properties of nanofluids at 293K

Nanofluid	Density (kg/m^3)	Specific heat (J/kgK)	Kinematic viscosity (m^2/s)	Thermal conductivity (W/mK)	Thermal expansion coefficient (1/K)
TiO_2-Water	1063.2	3902.5	0.000000982	0.6378	0.0001537
CuO-Water	1108.3	3754.3	0.000000943	0.6382	0.0001534
NiO-Water	1114.5	3744.6	0.000000937	0.6394	0.0001532

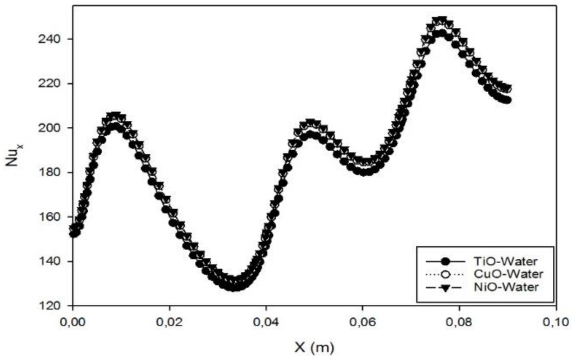

Figure 9. Local Nusselt number for different nanofluid

5. Conclusions

Present study is focused on numerical investigation of heat enhancement and fluid flow from a heated surface by using nanofluids and impinging jets. Effects of different Reynolds numbers, particle diameter and different types of nanofluids (TiO_2-water, CuO-water, NiO-water) on heat transfer and fluid flow were studied numerically. According to our constraints it is obtained that increasing jet velocities from the first phase to the third phase causes an increase of 49.9% on ANN but increasing jet velocities from the third phase to the fourth phase causes a decrease of 4.6% on ANN. Decreasing particle diameter from D_p=80nm to 10nm causes an increases of 2.9% between on ANN. These increase occurs 2.1% between D_p=40nm to 10nm. Using NiO-Water nanofluid causes an increase of 1% on ANN with respect to CuO and 2.8% with respect to TiO_2-water. Velocity of the third phase, D_p=10 nm and using NiO-water nanofluid shows better heat transfer performance. Research areas for future investigations can be investigation of effect of hybrid nanofluids with different base fluids on heat transfer with impinging jet geometry.

Acknowledgment

This work supported by the Adana Science and Technology University under Research Project (project no:16103021), Turkey.

Nomenclature

CP : Specific Heat (J/kgK)
ρ : Density(kg/m3)
φ : Nanoparticle volume fraction
μ : Dynamic viscosity(Pa.s)
Pr : Prandtl Number
Re :Reynolds Number
Nu_X : Local Nusselt number
k_{eff} :Effective Thermal Conductivity

References

1. Cakır, M.T, *Alamüna içeren Nanoakışkan kullanarak ısı borularının performanslarının iyileştirilmesi*, Journal of The Faculty of Engineering and Architecture of Gazi University, 2015. **30**: p.547-556.
2. Sun, B., Qu, Y., Yang, D., *Heat transfer of Single Impinging jet with Cu nonofluids*, Applied Thermal Engineering, 2016.**102**: p.701-707.
3. Teamah, M.A., Dawood M.M., Shehata A., *Numerical and experimental investigation of flow structure and behavior of nanofluids flow impingement on horizontal flat plate*, Experimental Thermal and Fluid Science, 2016. **74**: p.235-246.
4. Qu j., Wu H.Y., Cheng P.,*Thermal performance of an oscillating heat pipe with* Al_2O_3*-water nanofluids*, International Communication Heat and Mass Transfer, , 2010. **37**:p.111-115.
5. Chien, H.T., Tsia C.Y., Chen P.H., Chen P.Y., *Improvement on thermal performance of a disck-shape miniature heat pipe with nanofluid,* Proceedings of the fifth International Conference on Electric Packaging Technology, 2003,**17**:p.389-391.
6. Kang S.W.,Wei,W.C., Tsia S.H., Yang S.H., *Experimental Investigation of silver nano-Fluid on heat pipe thermal performance,* Applied Thermal Engineering, 2006. **26**: p.2377-2382.
7. Xuan Y., Li Q., *Heat transfer enhancement of nanofluids*, Int.Journal of Heat and Flouid Flow, 2000. **21**:pp.58-64.
8. Shang F.M., Liu D.Y., Xian H.Z., Yang Y.P., Du X.Z., *Flow and heat transfer characteristics of different forms of nanaometer particles in oscillating heat pipe*, Journal of Chemical Industry, 2007. **58**: p.2200-2204.
9. Manay E., Sahin B., Akyurek E.F., Comakli O. *Mikro kanallarda nanaoakışkanalrın kullanımı,* TMMOB MMO Mühendis ve Makina Dergisi, 2012. **53**: p.38-42.
10. Naphon P., Asssdamongkol P., Borirak T., *Experimental investigation of titanium nanofluids on the heat pipe thermal efficiency*, International Communication Heat and Mass Transfer, 2008. **35**: p.1316-1319.
11. Kilic, M., Çalışır, T., Başkaya, Ş, *Experimental and numerical study of heat transfer from a heated flat plate in a rectangular channel with an impinging Jet,* Journal of the Brazilian Society of Mechanical Sciences and Engineering, 2016**. 48**, p.1-16.
12. Kilic M., *Experimental and numerical study of heat transfer fro a heated flat plate in a rectangular channel with an impinging Jet*, PhD Thesis, Graduate School of Natural and Applied Science, Gazi Unıversity, Turkiye, Oct. 2013.
13. Corcione M., *Empirical correlating equations for predicting te effective thermal conductivity and dynamic viscosity of nanofluids.Energy Convers*. *Manag,* 2011. **52**(1), p.789-793.
14. Abdulvahitoğlu A, Evaluation of the fuel quality values of bay laurel ol as a biodiesel feedstock/title, Biofuels, 2018, **9**: p.95-100.
15. Abdulvahitoğlu A,Tüccar G., 2017, *Dizel Motorlarda Alternatif Yakıt Olarak Karpuz Çekirdeği Biyodizelinin Değerlendirilmesi,* Gazi Üniversitesi Mühendislik-Mimarlık Fakültesi Dergisi, 2017. **32**:p.211-216, 10.17341/gazimmfd.300610.
16. Abdulvahitoğlu A., Aydın K., *Performance and exhaust emission characteristics of a CI engine fueled with synthesized fuel blends,* Energy Education Science and Technology Part A: Energy Science and Research, 2012.**2**:p. 699-710.